ORIGINAL ARTICLE

JCSM Rapid Communications 2022; **5**: 130–145
Published online 14 January 2022 in Wiley Online Library (wileyonlinelibrary.com) **DOI:** 10.1002/rco2.57

Overexpression of thioredoxin-2 attenuates age-related muscle loss by suppressing mitochondrial oxidative stress and apoptosis

Huibin Tang[1,2], Michael Kim[1,2], Myung Lee[1,2], Kellie Baumann[1,2], Francesca Olguin[1,2], Hao He[1,2], Yoyo Wang[1,2], Bowen Jiang[1,2], Shuhuan Fang[1,2], Jinguo Zhu[1,2], Kun Wang[1,2], Hui Xia[1,2], Yang Gao[1,2], Harrison B. Konsker[1,2], Emmanuel A. Fatodu[1,2], Marco Quarta[3], Justin Blonigan[3], Thomas A. Rando[2,3] & Joseph B. Shrager[1,2]*

[1]*Division of Thoracic Surgery, Department of Cardiothoracic Surgery, Stanford University School of Medicine, 291 Campus Drive, Stanford, CA 94305, USA;* [2]*VA Palo Alto Healthcare System, Palo Alto, CA, USA;* [3]*Paul F. Glenn Laboratories for the Biology of Aging and Department of Neurology and Neurological Sciences, Stanford University School of Medicine, Stanford, CA, USA*

Abstract

Background Skeletal muscle mass is regulated by intracellular anabolic and catabolic activities. Increased catabolic activity can shift the balance towards net protein breakdown and muscle atrophy. Mitochondrial oxidative stress activates catabolism and is linked to muscle loss. Reducing mitochondrial oxidative stress is thus a plausible approach to prevent muscle atrophy. We tested this concept in age-dependent muscle atrophy by genetically overexpressing the mitochondrial antioxidant thioredoxin-2 (TXN2).

Methods We tested the functional role of TXN2 using ageing (n = 7–10 per group) and denervation (n = 3 per group) models in a transgenic mouse line that overexpresses TXN2. We investigated if overexpression of TXN2 blocks muscle loss in these models by examination of muscle weight, fibre size, and fibre number in young (~7 months) and aged (~26 months) TXN2-transgenic mice and controls. We studied the underlying mechanisms by mRNA and protein assays including transcriptomic profiling, western blot analysis, immunostaining, as well as succinate dehydrogenase, dihydroethidium, and terminal deoxynucleotidyl transferase dUTP nick end labelling staining.

Results Overexpression of TXN2 did not significantly alter the baseline skeletal muscle size, weight, fibre type distribution, or expression of mitochondrial respiratory chain components, but it did preserve muscle mass during ageing. The hindlimb muscle mass in aged TXN-transgenic mice was ~21–24% greater (in tibialis anterior, gastrocnemius/soleus combined, and tibialis anterior/extensor digitorum longus combined) than in age-matched controls (all $P < 0.05$). The reduction in both muscle fibre number (872 ± 206 vs, 637 ± 256 fibres in extensor digitorum longus muscle, $P < 0.05$) and muscle fibre size (1959 ± 296 vs. 1477 ± 564 μm^2 in tibialis anterior muscle, $P < 0.05$) seen in young vs. aged control muscles was not significant in young vs. aged TXN-transgenic mice (both $P > 0.05$). Transcriptomic analysis revealed that catabolic genes that are up-regulated in ageing muscle, including those subserving apoptosis and the ubiquitin-like conjugation system, were normalized by TXN2 overexpression. Further, overexpressing TXN2 suppressed oxidative stress and caspase-9/3-mediated apoptotic signalling in the aged muscle at the protein level. Although denervation and its effects have been considered a component of age-related muscle atrophy, TXN2 overexpression failed to attenuate atrophy in an acute denervation model (TXN-transgenic vs. control mice, $P > 0.05$), despite preventing denervation-induced oxidative stress and apoptosis.

Conclusions Mitochondrial oxidative stress appears to play a crucial role in effecting chronic age-dependent, but not acute neurogenic, muscle atrophy. Increased TXN2 protects muscle against oxidative stress-associated catabolic activity in ageing muscle and thus is a potential therapeutic approach to attenuate age-related muscle atrophy.

Keywords Ageing; Denervation; Oxidative stress; Muscle atrophy; Thioredoxin-2

Received: 17 June 2021; Revised: 22 November 2021; Accepted: 29 November 2021

**Correspondence to: Joseph B. Shrager, Division of Thoracic Surgery, Department of Cardiothoracic Surgery, Stanford University School of Medicine, 291 Campus Drive, Stanford, CA 94305, USA. Email: shrager@stanford.edu*

Introduction

Age-related loss of muscle mass and function, that is, sarcopenia, is a major health issue in the elderly. Sarcopenia causes frailty and increases both morbidity and mortality.[1] As life expectancy increases, sarcopenia-related health issues will continue to rise. Successful interventions against sarcopenia would preserve physical strength and improve both quality of life and longevity.

Skeletal muscle mass in healthy, mature muscle is maintained by balanced anabolic (e.g. protein synthesis) and catabolic (e.g. protein degradation and apoptosis) activities. Elevated catabolic activity in acute (e.g. nerve injury/denervation) or chronic (e.g. ageing) conditions shifts this balance towards muscle atrophy. Several signalling pathways that regulate muscle protein synthesis and degradation have been identified. IGF/Akt/mTOR is a well-known anabolic signalling pathway that promotes protein synthesis and muscle hypertrophy,[2] whereas the HDAC/myogenin, FoxO, and IKK/NFkB signalling pathways appear to facilitate protein degradation and muscle atrophy.[3–7] Closely associated with these molecular signalling pathways is a biochemical event, oxidative stress, that serves as a regulator of protein metabolism. It has been shown that oxidative stress is able to activate catabolic activity by inducing apoptosis and protein degradation in cultured myotubes.[8] Prolonged and excessive reactive oxygen species (ROS) is also linked to oxidative damage and protein degradation in human skeletal muscle.[9–16] For example, ageing increases oxidative damage to both DNA and proteins,[15] the expression of ROS-metabolizing catalase and Prx3, as well as proteins central to proteolysis in human muscle biopsies.[16] These findings suggest that oxidative damage may be involved in the pathogenesis of age-related muscle atrophy and that the up-regulated antioxidant genes are inadequate to counterbalance the increased ROS production. Muscle denervation, that is, loss of motor neuron innervation, is a circumstance promoting skeletal muscle atrophy through up-regulation of the ubiquitin-proteasome system via mechanisms involving HDAC/myogenin and FoxO.[3,5,7,17] Interestingly, both oxidative stress and denervation occur as muscle ages, and thus, each of these have thus been considered potential therapeutic targets for age-related muscle atrophy.[11,18–25]

Oxidative stress is subserved by increased levels of intracellular ROS, such as superoxide radical, hydroxyl radical, and hydrogen peroxide, as well as their derivatives such as reactive nitrogen species. ROS is produced primarily by the electron transport chain in the mitochondrial inner membrane during oxidative phosphorylation. Under physiological conditions, the level of ROS is maintained in homeostasis by mitochondria-resident antioxidant mechanisms, such as the thioredoxin cycle and the glutathione peroxidases (GPx). The mitochondrial redox system is composed of peroxiredoxins (Prx3/5), thioredoxin-2 (TXN2), and thioredoxin reductase. ROS superoxide radical is dismutated by mitochondrial superoxide dismutase (SOD2) and converted into hydrogen peroxide (H_2O_2). Approximately, 99.9% mitochondrial H_2O_2 is further detoxified by Prx3/5 (mainly) and GPx in a healthy cell.[26] A sustained, elevated level of ROS is harmful to cellular components (DNA, lipids, and proteins), inducing oxidative damage. Elevated ROS can directly oxidize proteins, reducing the function of the muscle contractile apparatus, and initiate proteasome-mediated protein degradation. Increased ROS can also trigger the release of cytochrome C, which further activates caspases and the apoptotic pathway.[27]

Because oxidative stress is triggered by ROS derived primarily from mitochondria, we hypothesized that *mitochondria-targeted* antioxidants (MTA) might detoxify ROS most efficiently, while minimizing side effects from interruption of ROS-mediated signal transduction. Indeed, a comparison of mitochondria-targeted, peroxisome-targeted, and nuclei-targeted expression of catalase—a metabolic enzyme that degrades H_2O_2—showed that the best protection against oxidative stress resulted from mitochondria-targeted catalase.[28] Some MTAs, such as SS-31[29] and XJB-5-131,[30] have been shown to protect muscle mass or function with age, although another report found that SS-31 treatment affected neither contractile force nor muscle mass in aged mice.[31] Therefore, there remains controversy over the effect of MTAs on muscle ageing.

Beyond these synthetic MTAs, genetic overexpression of ROS-metabolizing enzymes, mitochondria-targeted catalase, decreased oxidative stress, and extended life span,[32] increased skeletal muscle-specific force,[28] attenuated the age-dependent reduction in muscle mitochondrial function and energy metabolism,[33] and prevented cardiac ageing.[34] However, catalase can only decompose H_2O_2, one of the ROS molecules, which limits its effect in reducing oxidative stress. For example, the defects in Drosophila that underexpressed Prx—massive apoptosis, reduced lifespan—were not offset by mitochondria-targeted catalase.[35] In contrast to catalase, TXN2 is an endogenous mitochondrial antioxidant that does not directly target H_2O_2. TXN2 promotes the decomposition of H_2O_2 by reducing mitochondrial Prx3 that is extremely effective at scavenging peroxides, and is the major mitochondrial H_2O_2 scavenging enzyme.[26]

To date, two TXNs have been identified—TXN1 and TXN2. Both are small (~12 kDa), redox-active proteins containing an evolutionarily conserved redox motif, Trp-Cys-X-Pro-Cys. TXN1 is located in the cytosol, whereas TXN2 is a mitochondria-specific protein. TXNs diminish ROS-induced damage by (i) participating in the decomposition of H_2O_2 by reducing Prx and (ii) reducing oxidized proteins by transferring electrons from TXNs to their target proteins, for example, NFkB[36] and HDAC4.[37]

DOI: 10.1002/rco2.57

Mitochondrial TXN2 plays an important role in regulating mitochondrial oxidative stress (MOS) and apoptosis. TXN2 is essential for cell survival and plays a crucial role in regulating mitochondrial apoptosis.[38,39] In cultured cells and a haploinsufficiency mouse model, reduction of TXN2 led to ROS accumulation, cytochrome C release, and apoptosis.[38,40] Complete deletion of the TXN2 gene in mice caused massive apoptosis and early embryonic lethality.[41] Cardiac muscle-specific knockout of TXN2 led to the disruption of mitochondrial ultrastructure and function, accumulation of mitochondrial ROS, and cardiomyocyte apoptosis.[42] In Drosophila, lack of TXN2 reduced their lifespan, whereas overexpression increased the tolerance to oxidative stress.[43] Mitochondria isolated from TXN2-transgenic mice were able to attenuate peroxide-induced necrotic and apoptotic changes via resisting mitochondrial permeability transition.[44] Overexpression of TXN2 was also able to improve the function of various tissues/organs including the brain, retina, and heart.[42,45–47]

However, the functional role of TXN2 in the development or ageing of skeletal muscle has not been studied. We felt it plausible to speculate that increasing TXN2 may reduce oxidative stress-associated muscle loss during ageing. With a TXN2-transgenic mouse model, we indeed found that overexpression of TXN2 attenuated muscle mass during ageing. Mechanistic studies revealed that overexpression of TXN2 suppressed the up-regulation of oxidative stress and catabolic activity (e.g. apoptosis) associated with ageing in skeletal muscle. Overexpression of TXN2 did not, however, mitigate acute muscle atrophy induced by short-term denervation. Therefore, MOS and its associated apoptotic fibre damage appear to play a more prominent role in ageing muscle loss than in acute denervation-induced muscle atrophy. Our findings from the current, cross-sectional study suggest that increasing TXN2 represents a potential approach to preserve muscle mass during ageing.

Materials and methods

Animals and muscle denervation

The animal care and experimental procedures followed a protocol approved by the Veterinary Medical Unit at the VA Palo Alto Healthcare System. TXN2 transgenic mice, on a C57BL/6 background, were initially generated in the laboratory of Dr. Dean P. Jones at Emory University. In this transgenic line, there is ubiquitous overexpression of human TXN2, driven by a chicken β-actin gene (CAG) promoter. This colony was further expanded in our animal facility. Hemizygous TXN2 mice were bred with each other to generate homozygous (Homo, tg/tg), hemizygous (Hemi, tg/+), and control (Ctl, +/+) mice for use in the current experiments. Genotyping was performed as described previously,[44] with primers: 5′-GCC AAT CAG CTT CTT CAG GAA GGC-3′ and 5′-CAC CAT GGC TCA GCG ACT TCT TCT-3′. These primers do not identify endogenous mouse Trx2.

The baseline phenotype was analysed with control, hemizygous, and homozygous female mice at ~7 months old. Mice were euthanized at the indicated age, and hindlimb muscles were immediately harvested, weighted, and frozen in liquid nitrogen for protein analysis. Tibialis anterior (TA) muscle was embedded in optimal cutting temperature (OCT) compound for histology and immunostaining. Female mice were used in the age-related studies, and the age groups included young controls at 7.5 ± 1.5 months (n = 7, bodyweight 34 ± 7 g), young TXN2-transgenic mice at 6.9 ± 1.9 months (n = 9, bodyweight 40 ± 9 g), aged controls at 26.5 ± 1.3 months (n = 10, bodyweight 27 ± 7 g), and aged TXN2 transgenic mice at 26 ± 4 months (n = 6, bodyweight 35 ± 10 g).

Denervation was performed in adult mice (9 months old, n = 3 per group). The procedure of sciatic nerve denervation was the same as described previously.[3] Briefly, the animals were anaesthetised with ketamine (100 mg/kg) and xylazine (10 mg/kg). Following an aseptic procedure, an incision was made, and a 5 mm segment of sciatic nerve trunk was removed at the mid-thigh level from the anaesthetised mice. The mice were carefully monitored post-surgically. Both innervated (contralateral) and denervated muscles from the lower legs were harvested 14 days post-denervation.

RNA extraction, quantitative PCR, microarray, and data analysis

Total RNA was extracted from the gastrocnemius muscle, and microarray was performed at the Stanford University core facility. Total RNA was extracted by TRIzol reagent (ThermoFisher Scientific, USA) and used for quantitative PCR and microarray analysis. Gene expression levels were detected by quantitative PCR. Total RNA was converted to cDNA with SuperScript II First-strand Synthesis System (ThermoFisher Scientific, USA). The cDNA mixture (about 1/20) was used as the template for the PCR reactions. Quantitative PCR was performed by using the Dream Taq PCR master mix kit (ThermoFisher Scientific, USA) with an ABI7100 instrument (Applied Biosystems, USA). The expression of γ-actin was used as the house-keeping gene for normalization. Comparative Ct ($\Delta\Delta$Ct) method was used to show the fold change of mRNA expression. The primers used for quantitative PCR are listed in the supporting information. Gene expression microarray was also performed in the Stanford University core facility. Data were analysed by GeneSpring GX and DAVID bioinformatics

software (http://david.ncifcrf.gov/content.jsp?file=citation.htm). The changes in mRNA expression between young and aged contro mice were further compared with the changes between the aged control and aged TXN2-transgenic mice, and the commonly regulated genes were then subjected to signal pathway mining by DAVID bioinformatics. UP_key words were used to organize the altered signalling pathways.

Protein extraction and western blot analysis

Protein expression and post-translational modifications including oxidation and phosphorylation were detected by western blotting analysis following standard procedures. Briefly, total protein was extracted from gastrocnemius muscle by RIPA buffer (140 mM NaCl, 25 mM Tris–HCl, 1 mM EDTA, 0.5 mM EGTA, 1 mM PMSF, 1 mM NaF, 1% Triton X-100, 0.1% SDS, 0.1% protease inhibitors cocktail, and pH adjusted to 7.4). Protein concentration was quantitated by a DC protein assay kit (Bio-Rad, USA) following the manufacturer's instructions. Ten micrograms of total protein were loaded onto 4–12% SDS-PAGE gels and run for 1 h at 120 V, and then transferred to nitrocellulose membranes at 25 V for 1 h for antibody detection. Antibodies (Mitoprofile) against the components in the mitochondrial respiratory chain were purchased from Abcam, UK. The anti-nitrotyrosine antibody was from Millipore, USA. The other antibodies used in this study were purchased from Cell Signalling Technologies. Primary antibodies were incubated with the membrane overnight at 4°C. After washed three times in 1 X PBST (1 × PBS with 0.1% Tween 20), the membrane was incubated with HRP conjugated secondary antibody for 2 h at room temperature. Clarity ECL (Bio-Rad, USA) was used to develop the membrane in ChemiDoc (Bio-Rad, USA). The grey density of the western blotting bands was quantitated by ImageJ (http://imagej.nih.gov/ij/index.html).

Immunohistochemistry, dihydroethidium staining, and succinate dehydrogenase staining

Immunohistochemistry was performed with a VECTASTAIN Elite ABC-HRP Kit (Vector Laboratories) following the supplier's instructions. Briefly, cryosections were fixed in cold acetone for 10 min at −20°C, followed by 2% paraformaldehyde (PFA) for 5 min. Primary antibody, anti-cleaved caspase-3 (Cell Signalling Technologies, USA), was incubated with tissue sections at 4°C overnight, followed by biotin-conjugated secondary anti-rabbit antibody and Avidin-HRP complex, and the chromogenic signals were generated by 3, 3′-diaminobenzidine.

The muscle cell membrane was visualized by wheat germ agglutinin (WGA) staining. Muscle cryosections were fixed with 4% PFA for 15 min. After 1 X PBS wash, the fixed tissue sections were incubated with 10 μg/mL WGA conjugates (Alexa 488, green) for 10 min at room temperature.

Succinate dehydrogenase (SDH) staining was performed on cryosections from OCT-embedded muscle tissues as described previously.[4] SDH activity was visualized by SDH-dependent formation of purple-blue formazan pigment. Briefly, fresh muscle tissues were embedded in OCT and frozen in liquid nitrogen-cooled isopentane. Cryosections (18 μm) without fixation were incubated within 0.1 M phosphate buffer, pH 7.6, 5 mM EDTA, pH 8.0, 1 mM KCN, 21.8 mg/mL sodium succinate, and 1.24 mg/mL nitroblue tetrazolium for 20 min at room temperature. The tetrazolium was further converted to formazan pigment after receiving hydrogen, marking the location and activity of the SDH enzyme. Sections were then rinsed, dehydrated, and mounted.

Free radicals were stained by dihydroethidium (DHE) following the supplier's instructions. DHE was stained in cryosections (20 μm) that were cut from freshly prepared, OCT-embedded snap-frozen tissue blocks. DHE (Invitrogen, USA) was reconstituted in anhydrous DMSO (Sigma-Aldrich, USA) at a stock concentration of 10 mM. The staining solution was prepared freshly before use by 1 to 1000 dilution of the stock DHE solution with PBS. The DHE/PBS solution was placed over cryosections and incubated for 10 min in a dark chamber. The staining was terminated by rinsing in PBS3 times. Slides were mounted in Prolong Gold anti-fading reagent (Invitrogen, USA).

All these stainings were performed with TA muscle cryosections. Fluorescent images were taken by fluorescent confocal microscopy (Leica, Germany), and chromogenic staining (3, 3′-diaminobenzidine and SDH) was visualized and imaged by a BZ-9000E microscope (Keyence, Japan).

Muscle fibre cross-sectional area and fibre number

Cross-sections of the same location of each muscle were created for the measurement of cross-sectional area (CSA). Briefly, TA muscle cryosections were fixed with 4% PFA, and the cell membrane was stained with WGA (ThermoFisher, USA). The CSA was measured by ImageJ software, as described previously.[3] Approximately 250 fibres per region, two (*Figure* 2), or three regions (*Figure* 6) per muscle, were measured. The total muscle fibre number in extensor digitorum longus (EDL) muscles was counted after WGA staining, young control: n = 6; aged control: n = 5; young TXN2-tg: n = 9; aged TXN2-tg: n = 5.

Plasmid contraction, cell culture, and gene transfection

TXN2-GFP was constructed by PCR amplification of the cDNA of mouse TXN2 and ligation into an AAV-RSVeGFPH1 vector (a gift from Dr. Mark A. Kay, Stanford) at the BamHI site. The primers used were forward: TTTATCGGATCCATGGCTCAGCGGCTCCTCCTG; reverse GTCTTTAGGATCCCCGCCAATCAGCTTCTTCAGGAAGGC. The construct was then transfected into cultured C2C12 cells with lipofectamine2000 (Invitrogen, USA), together with a puromycin-resistant plasmid at a 10 to 1 ratio. A stable cell line was selected with puromycin and purified with fluorescence-activated cell sorting based on GFP signal.

Both the parental and the TXN2-transfected C2C12 cells were cultured with DMEM medium supplemented with 10% foetal bovine serum and 100 IU/mL penicillin and 100 μg/mL streptomycin. C2C12 myoblasts were induced to differentiation in DMEM supplemented with 5% horse serum. Cultured cells were incubated with 500 nM Mitotracker (ThermoFisher, USA) at 37°C for 1 h to visualize mitochondria. Differentiated myotubes were also treated with either H_2O_2 (Sigma, USA) at 40 μm or same volume of water for 24 h.

Terminal deoxynucleotidyl transferase dUTP nick end labelling assay

DNA breaks were detected with the Click-iT Plus terminal deoxynucleotidyl transferase dUTP nick end labelling (TUNEL) assay (Invitrogen, USA) following the supplier's instructions. Briefly, cryosections of TA/EDL muscles were fixed with 4% PFA for 15 min. EdUTP (dUTP modified with a bioorthogonal alkyne moiety) nucleotides were incorporated at the 3′-OH ends of fragmented DNA by a TdT (terminal deoxynucleotidyl transferase) enzyme-mediated reaction, and the alkyne moiety was detected through covalently binding with an Alexa Fluor. Nuclei and cell membranes were counterstained by DAPI and WGA, respectively. TUNEL index was calculated as the percentage of cells that showed TUNEL-positive signal (at least one of the nuclei being positive) over total cells in the image. Four images were taken from the stained cryosections of each gastrocnemius muscle, and three muscles/animals per group were included in the calculation and statistics.

Statistics

A Student's *t*-test was used to evaluate the statistical significance of the difference between any two groups, and a $P < 0.05$ was considered as statistically significant. Error bars in bar graphs represent standard errors of the mean. To estimate the adjusted age effect on CSA, a mixed-effects model was fitted, in which animal age, group, the interaction of age by group, and by fibre region were included as the fixed effects. The animal subject was set as the random effect in the model to adjust the correlation among fibre area measurements from the same animal. Model effects were tested by the *F*-test. The multivariate analysis was performed using SAS Version 9.4 (SAS Institute Inc. NC, USA). In all statistical analyses, a two-sided α-level of 0.05 was considered statistically significant.

Results

Overexpression of TXN2 does not significantly alter the baseline phenotype of skeletal muscle

Increased expression of TXN2 in the skeletal muscle of the TXN2 transgenic mice (mice with ubiquitous TXN2 overexpression) was confirmed (*Figure* 1A). To examine whether the increased expression of TXN2 in skeletal muscle changed the phenotype of adult skeletal muscle, we compared the muscle mass, fibre composition, and the expression of the components of the mitochondrial reparation chain between control (Ctl), hemizygous (TXN2 tg/+), and homozygous (TXN2 tg/tg) mice (~7 months). Overexpression of TXN2 did not significantly alter the bodyweight or muscle weight (*Figure* 1B and 1C). The muscle fibre types and distribution pattern of glycolytic and oxidative fibres, revealed by SDH staining, were also similar between the controls and the transgenic mice, as demonstrated in TA muscles (*Figure* 1D). The protein expression levels of the components of the mitochondrial respiratory chain, such as complexes I (CI: NDUFB8), II (CII: SDHB), III (CIII: UQCRC2), IV (CIV: MTCO1), and V (CV: ATP5A), also remained the same between the control, hemizygous, and homozygous TXN2-transgenic mice (*Figure* 1E).

Taken together, it appears that increasing TXN2 in skeletal muscle does not significantly change the baseline phenotype in adult skeletal muscle.

Overexpression of TXN2 attenuates age-related muscle loss

We further employed TXN2-transgenic mice to test the hypothesis that increasing mitochondrial antioxidant TXN2 would attenuate age-related muscle loss (*Figure* 2A). Because we observed no difference in phenotype between the hemizygous and homozygous muscle, we used homozygous TXN2 mice in the remaining experiments unless otherwise specified. We examined the muscle weight in young (~7 months) and aged (~26 months) mice, with and without

Figure 1 Overexpression of TXN2 does not alter the baseline phenotype of skeletal muscle. (*A*) TXN2 is overexpressed in skeletal muscle. The expression of TXN2, both the endogenous and the overexpressed, was confirmed by western blot analysis. TXN2 is increased in the hemizygous (tg/+) and homozygous (tg/tg) transgenic mice. Beta-actin protein was detected as the loading control. (*B* & *C*) Bodyweight (*B*) and muscle weight (*C*, gastrocnemius, and tibialis anterior) were similar between the control, hemizygous (tg/+), and homozygous (tg/tg) mice (n = 6 each). (*D*) The distribution pattern of the oxidative (SDH+) and glycolytic (SDH−) fibres in skeletal muscle, shown by SDH staining, is similar between control, hemizygous, and homozygous mice (n = 3). (*E*) The components of the mitochondrial electron transporter chain are expressed at a similar level between control, hemizygous, and homozygous mice (n = 3 per group, representatives showed). Quantitation of the expression of each mitochondrial protein was shown by averaging the plotting profiles (n = 3) from ImageJ. SDH, succinate dehydrogenase; TA, tibialis anterior.

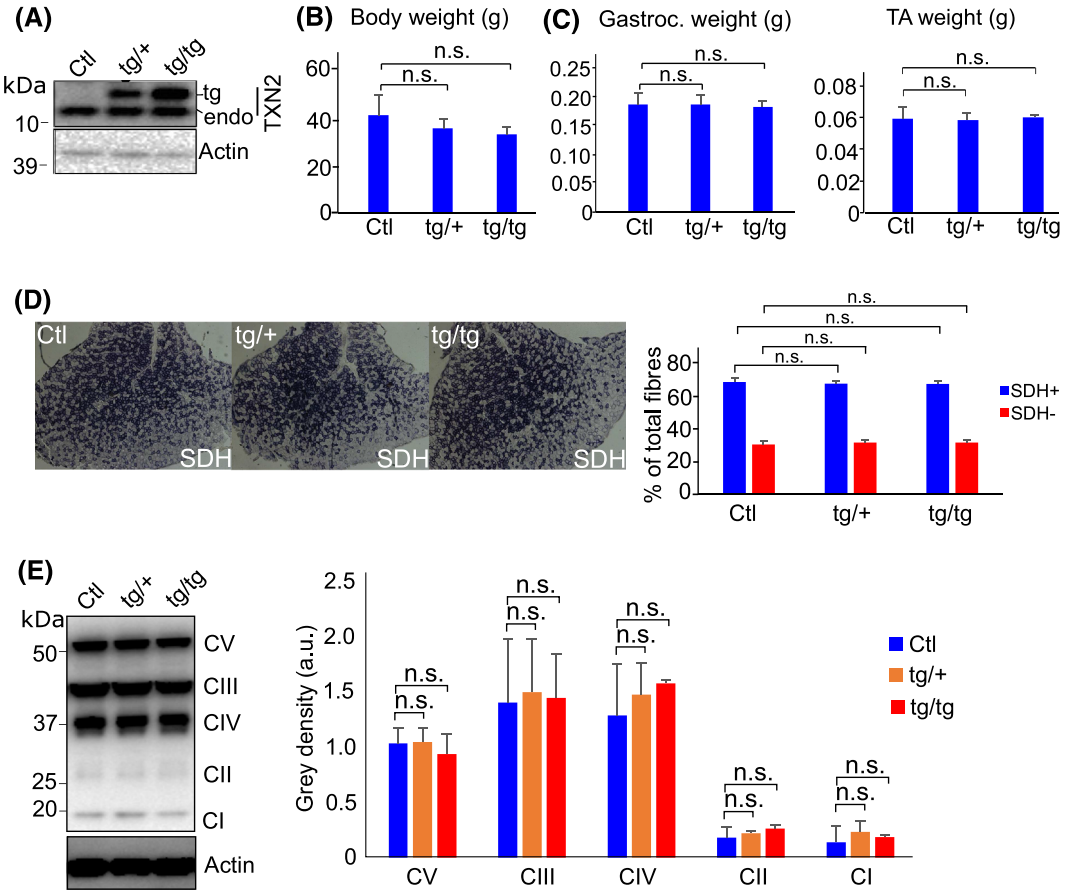

TXN2 overexpression. The muscle weight (normalized to body weight) was similar in young mice between the controls and TXN2 transgenic mice. In the aged mice, the muscle weight was significantly higher in the TXN2-transgenic than the control mice, with a ~22% increase in TA/EDL (T/E), ~24% increase in gastrocnemius/soleus (G/S) muscles, and a 21% increase in TA muscle (*Figure* 2B and Supporting Information, *Figure* S1). In contrast, there was no significant weight difference of heart or kidney between the controls and the transgenic mice at either age (*Figure* 2C). Muscle fibre number was counted in EDL muscle. An age-dependent decline (~27%, $P < 0.05$) in muscle fibre number, from 872 ± 206 fibres in young EDL muscle to 637 ± 256 fibres in the aged controls, was observed in control mice, but not in the TXN2-transgenic mice (young vs. aged: 833 ± 201 vs. 878 ± 57 fibres, $P > 0.05$). The muscle fibre number was significantly higher in the aged TXN2-transgenic mice than age-matched controls (*Figure* 2D). Also, there was a significant age-dependent reduction (~25%, $P < 0.05$ vs. young) in mean muscle fibre size (CSA) in the control mice, from 1959 ± 296 μm^2 in the young TA muscle to 1477 ± 564 μm^2 in the aged, but not in TXN2-transgenic mice that have 1753 ± 286 μm^2 in the young and 1435 ± 466 μm^2 in the aged (~18% reduction, $P > 0.05$ vs. young) (*Figure* 2E and 2F), indicating that TXN2 overexpression ameliorated the reduction rate of fibre size during ageing. To be certain of this finding, we also used a mixed-effects multivariate model (*Table* 1) in which each individual fibre was analysed as an observation. In this analysis, we examined the average muscle fibre CSA of TA muscle in two different regions (randomly selected, $P < 0.01$), each containing approximately 250 fibres. Significant age-dependent reduction of fibre CSA in

Figure 2 Overexpression of TXN2 attenuates age-related muscle loss. *(A)* A schematic diagram showed the use of TXN2 transgenic mice to overcome the increased ROS during muscle ageing. *(B)* TXN2 overexpression attenuated the age-dependent reduction of muscle weight. Gastrocnemius and soleus muscles (G/S), and tibialis anterior and EDL muscles (T/E) were weighted and normalized to body weight. Young: $n = 7$; aged: $n = 9$; young TXN2: $n = 9$; aged TXN2: $n = 6$, $P < 0.05$. *(C)* Overexpression of TXN2 did not affect the weight of the heart and kidney in the control and the TXN2-transgenic mice at both young and aged ages. Young: $n = 7$; aged: $n = 9$; young TXN2: $n = 9$; aged TXN2: $n = 6$. *(D)* TXN2 overexpression attenuated the age-dependent loss of muscle fibres. Muscle fibre numbers in EDL muscles were counted, young: $n = 6$; aged: $n = 5$; young TXN2: $n = 9$; aged TXN2: $n = 5$; $P < 0.05$. *(E)* Muscle fibre size, cross-sectional area (CSA), was measured by ImageJ software. Approximately 500 fibres per muscle from two different regions were measured. Young: $n = 7$; aged: $n = 6$; young TXN2: $n = 4$; aged TXN2: $n = 5$, $P < 0.05$. *(F)* TXN2 overexpression did not alter the distribution pattern of muscle fibre size between the young and aged, in the control and the TXN2-transgenic mice. Data were shown with the average percentage of muscle fibre in each categorized fibre size. Young: $n = 7$; aged: $n = 6$; young TXN2: $n = 4$; aged TXN2: $n = 5$. ROS, reactive oxygen species.

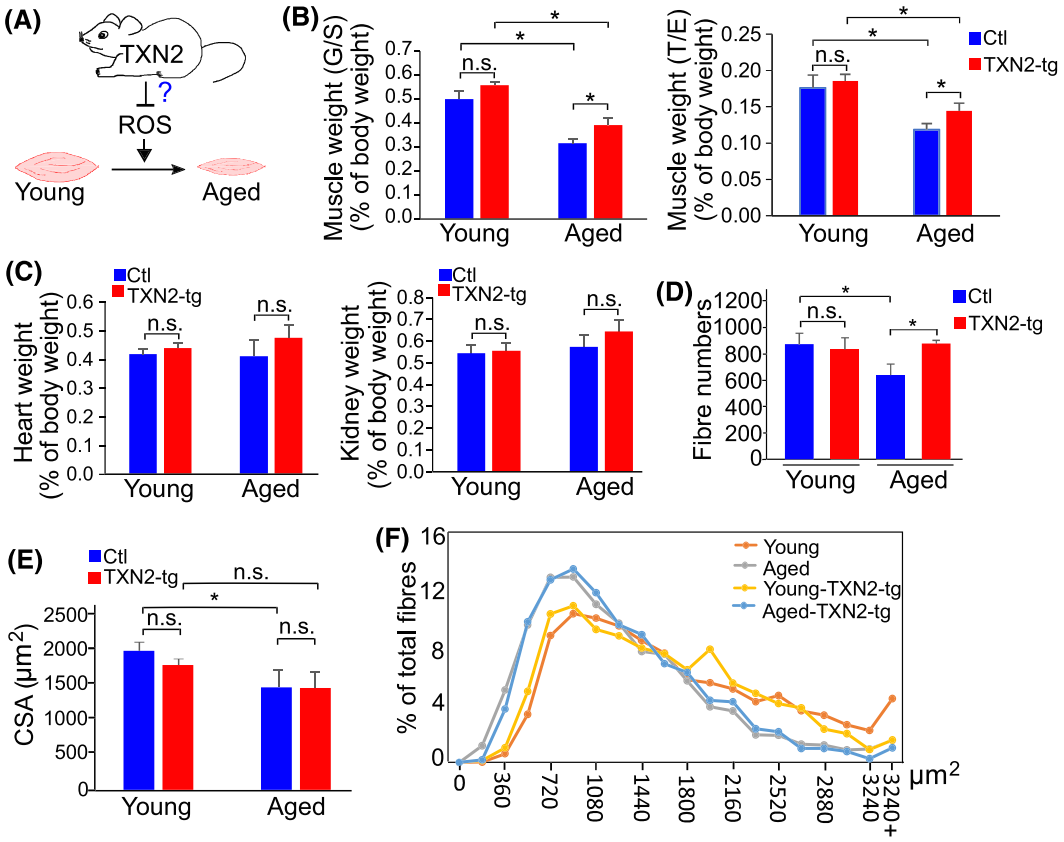

control mice was identified ($P = 0.05$) after adjustments of confounding from other factors, whereas there was no difference between young and aged-TXN2 transgenic mice, young TXN2, and young controls, nor any other comparisons (*Table* 1).

In sum, increasing TXN2 in skeletal muscle ameliorated age-related fibre loss and fibre atrophy.

Increasing TXN2 attenuates the transcriptional up-regulation of apoptosis-related and atrophy-related genes in aged skeletal muscle

To investigate how TXN2 protects skeletal muscle mass during ageing, we performed gene expression arrays on skeletal muscle from control and transgenic mice at young and aged ages. Transcriptomic expression profiles were analysed by GeneSpring and DAVID bioinformatics tools. We found that increasing TXN2 normalized the altered expression of several subsets of genes: some age–up-regulated genes were down-regulated by TXN2 overexpression, whereas some age–down-regulated genes were up-regulated by TXN2 overexpression (*Figure* 3A). The genes for which expression was normalized by TXN2 in aged muscle were subjected to pathway mining by DAVID bioinformatics software. As shown by the functional annotation with UP (UniProtKB) keywords (*Figure* 3A, right panel), genes involved in the categories 'oxidoreductase' and 'disulphide bond' were down-regulated in the aged control muscle but not in the aged TXN2-overexpressed muscle. Among the signalling pathways that are up-regulated in

DOI: 10.1002/rco2.57

Table 1 Mixed-effects multivariate model for muscle fibre area (CSA) of mice

Effect contrast[b]	Mixed-effects model estimates[a]		
	Difference of fibre area	Standard error	*P* value[c]
Age: Young vs. Aged	327.62	161.53	**0.04**
Group: Ctl vs. TRX2	129.69	161.50	0.42
Region: 1 vs. 3	267.08	15.38	<**0.01**
Age*group			
Ctl_Young vs. Ctl_Aged	400.61	206.10	**0.05**
TRX2_Young vs. TRX2_Aged	254.63	248.77	0.31
Ctl_Young vs. TRX2_Young	202.68	241.54	0.40
Ctl_Aged vs. TRX2_Aged	56.70	214.53	0.79

[a]Animal subject was set as a random effect to adjust the intra-correlation among fibre size measures from the same animal; difference of fibre area presented in the table were the average differences of muscle fibre cross-sectional area (CSA) between compared groups.
[b]The fixed effects (covariates) in the model included Age [young, aged], Group [Ctl, TRX2], Region [1, 3], and interaction of Age × Group. Ctl, control group. CSA from two different regions (1 and 3) of TA muscle were measured.
[c]*P* values obtained from *F*-test on effects.

the aged muscle but normalized by overexpression of TXN2, two are involved in catabolic activities: the apoptosis and ubiquitin-like conjugation pathways. As shown in *Figure* 3B, the genes involved in apoptotic and the ubiquitin-like conjugation pathways were induced in aged muscle, but that induction was attenuated by the overexpression of TXN2. The expression pattern of some of the genes involved in these catabolic pathways was further validated by quantitative PCR (*Figure* 3C).

To summarize, TXN2 overexpression partially normalized the age-dependent regulation of gene expression, helped to maintain the cellular redox activity, and suppressed the expression of genes involved in the apoptotic and ubiquitin-like conjugation pathways that are linked to proteolysis in aged muscle. The TXN2-dependent inhibition of the age–up-regulated catabolic genes appears to contribute to the protective effect of TXN2 against age-related skeletal muscle loss.

TXN2 overexpression inhibits oxidative stress and apoptotic changes in aged skeletal muscle and cultured myotubes

To further validate the apoptotic and ubiquitin-mediated changes indicated by the above mRNA expression profiles, we measured oxidized protein levels to examine the effect of the overexpressed TXN2 on oxidative stress in skeletal muscle. Western blot analysis (*Figure* 4A and 4B) shows that oxidized proteins (quantified by nitrotyrosine and 4HNE) were increased in the aged controls, but not in the aged TXN2-overexpressing mice (*Figure* 4A and 4B). Similarly, the apoptotic markers, cleaved caspase-3, and cleaved caspase-9, were both increased in aged muscle, but this age-dependent induction was near-completely blocked by TXN2 overexpression, indicating that overexpression of TXN2 efficiently suppressed age-dependent induction of mitochondrial/intrinsic apoptotic changes (*Figure* 4A and 4B). Protein ubiquitination also increased in the aged controls, but not in the TXN2 transgenic mice. The components of the mitochondrial electron transport chain complex, such as CV (ATP5A), CIII (UQCRC2), and CI (NDUFB8), were up-regulated during ageing, and this age-dependent up-regulation was suppressed in the TXN2-transgenic mice. Lastly, a mild but significant induction of TXN2 protein was observed in the aged muscles as compared with the young controls, perhaps reflecting a cellular homeostatic effort to counteract the age-induced increase in oxidative stress by up-regulating TXN2.

To visualize TXN2's effect on apoptosis in aged skeletal muscle, we also performed immunostaining to examine cleaved/active caspase-3 (Cle. Caspase-3) and TUNEL assay to detect DNA strand breaks. The expression of age-induced cleaved caspase-3 was significantly reduced in the aged TXN2-transgenic mice, compared with age-matched aged controls (*Figure* 4C). TUNEL index—the percentage of cells with TUNEL-positive signals out of total cells examined—was also induced in aged muscles, but it was significantly reduced in aged TXN2-overexpressed muscles, compared with aged controls (*Figure* 4D).

The protective effect of TXN2 against apoptotic changes in muscle was further validated in cultured muscle cells. We engineered a GFP-tagged TXN2 gene construct and established a stable C2C12 myogenic cell line expressing TXN2-GFP (*Figure* 5A). The mitochondria-specific distribution of TXN2-GFP was visualized by co-localization of TXN2-GFP with MitoTracker, a mitochondria-specific marker (*Figure* 5B). Further, we treated cultured control and TXN2-GFP myotubes with H_2O_2 (40 μM) for 24 h. Myotubes with overexpressed TXN2 demonstrated less protein ubiquitination and less activation of the apoptotic marker cleaved caspase-3 after H_2O_2 exposure than was seen in control cells (*Figure* 5C and 5D).

TXN2, then, is a potent inhibitor of oxidative stress and apoptotic changes in muscle cells both *in vivo* and *in vitro*.

Figure 3 Global gene expression profiling reveals that overexpression of TXN2 partially normalizes age-dependent gene expression. (*A*) Schematic diagram to show the gene profiling and data analysis. Transcriptomic profiling was performed with young, aged, and aged TXN2-overexpressed muscles (n = 3). GeneSpring software was used to analyse the statistics and fold changes. DAVID bioinformatics tool was used to mine the signalling pathways. Left panes showed the top, significantly altered signalling pathways categorized by UP keywords. TXN2 overexpression partially normalized altered signallings that were either up-regulated or down-regulated during ageing. (*B*) Genes participated in apoptotic and ubiquitin-like conjugation pathways. Fold changes in gene expression were listed. (*C*) The mRNA expression of genes involved in apoptosis and Ubl signalling was further validated by quantitative PCR, fold changes were shown. n = 3, $P < 0.05$.

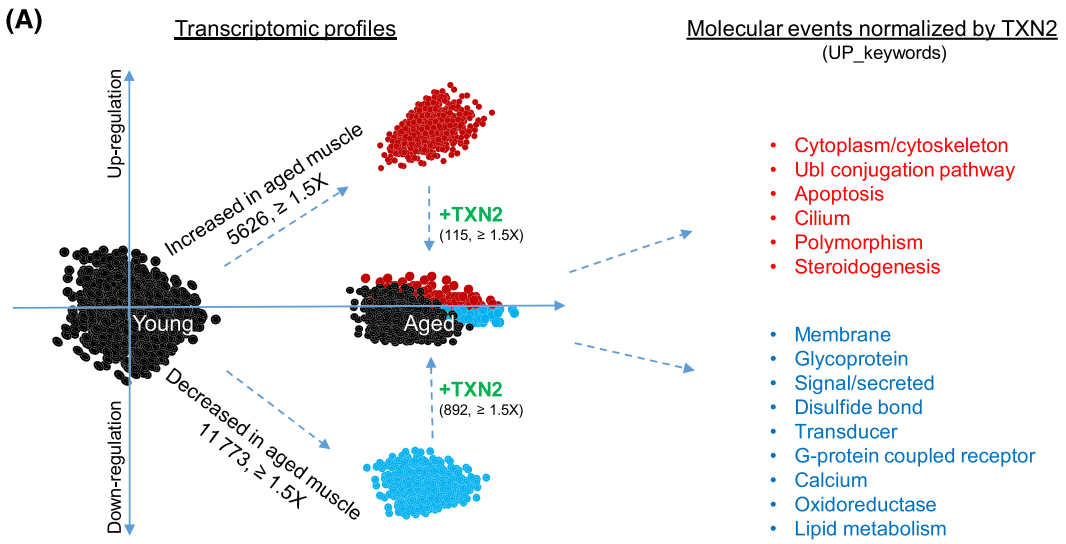

(B)

	Genes	F.C. Aged/Young	F.C. TXN2Aged/Aged
Apoptosis	Cradd	7.45	0.45
	Kcnip3	1.83	0.64
	Dido1	1.96	0.57
	Cdkn2a	7.06	0.55
	Hip1r	4.01	0.63
	Ntn1	4.34	0.67
	Tnfaip8	3.34	0.39
Ubl conjugation	Cul4a	3.08	0.54
	Ccnf	6.80	0.45
	Cdkn2a	7.06	0.55
	Herc3	6.50	0.53
	Herc6	1.77	0.59
	Uba1y	3.88	0.67
	Ube2l6	3.10	0.56

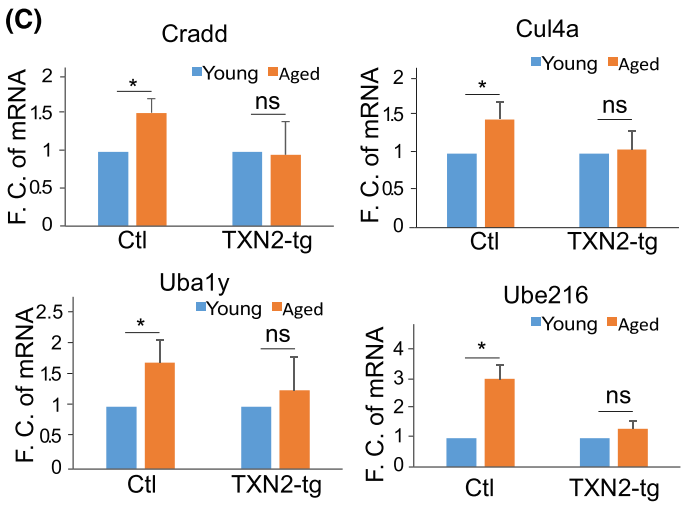

Overexpressing TXN2 does not attenuate muscle loss in acute neurogenic muscle atrophy induced by denervation

Because denervation occurs in aged skeletal muscle and is understood to be a subevent that contributes to ageing muscle atrophy[20–25,48] and because muscle denervation increases oxidative stress,[49–52] we opted to explore whether the protective effect of TXN2 against muscle loss in aged muscle may be in part related to attenuation of denervation-induced oxidative stress and muscle atrophy. To test this, we performed hindlimb denervation by sectioning the sciatic nerve in control and the TXN2-overexpressing mice and studied them after 14 days (*Figure* 6A). The weight and fibre size of the innervated and denervated muscles in control and TXN2-transgenic (hemizygous and homozygous) mice were compared. As shown in *Figure* 6B and 6C, denervation led to a similar degree of muscle atrophy in control and TXN2-transgenic mice. This was evident in both a lack of impact upon muscle weight (both the gastrocnemius and TA

Figure 4 Overexpression of TXN2 suppresses age-induced oxidative stress and apoptosis in skeletal muscle. (*A* & *B*) TXN2 overexpression suppressed the age-dependent induction of protein oxidation and ubiquitination, apoptotic markers, and the components in the mitochondrial electron transporter chain. (*A*) Western blot analysis was performed to examine the protein expression. (*B*) The grey density of the detected protein bands was quantitated and normalized to total protein (pons) to show the protein expression levels. Arbitrary unit (a.u.). $n = 3$ for young and young-TXN2, $n = 4$ for aged and aged-TXN2., $^*P < 0.05$. (*C*) Overexpression of TXN2 reduced the age-dependent induction of cleaved caspase-3 in skeletal muscle fibres. Gastrocnemius muscle was used for immunohistochemistry. Grey density was quantitated by ImageJ. Representative images were shown. The arrows indicated the positively stained cells, while the arrowheads indicated the positively stained nuclei. Scale bar = 50 μm. ns, no statistical difference; $n = 3$, $^*P < 0.05$. (*D*) Overexpression of TXN2 significantly reduced the DNA damage in aged muscle. Nuclear DNA breaks were shown by TUNEL assay performed on TA and EDL muscles. The TUNEL index was defined as the percentage of muscle fibres with positive nuclear staining over the total muscle fibres per image. Representative images were shown, and the arrows indicated the positively stained cells. Approximately 80–120 fibres per image, four images per sample, and three samples per group were counted. Scale bar = 50 μm. ns, no statistical difference; $^*P < 0.05$.

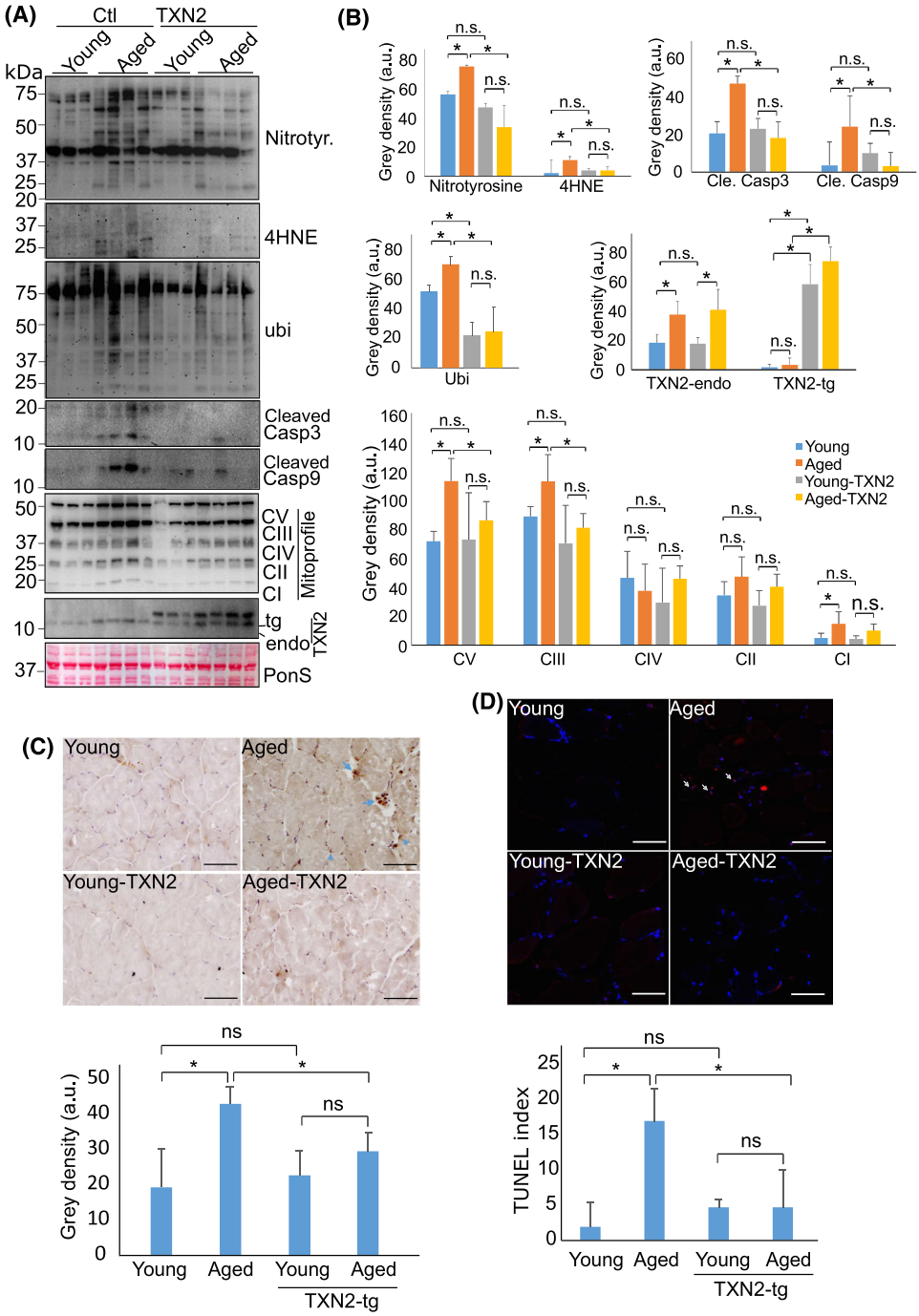

DOI: 10.1002/rco2.57

Figure 5 Overexpression of TXN2 suppresses H_2O_2-induced oxidative stress and apoptosis in cultured myotubes. (*A*) Establishing a stable C2C12 cell line expressing TXN2-GFP fusion protein. A schematic diagram showed the construct that expresses TXN2-GFP fusion protein (top left) and a representative image showed the establishment of the TXN2-GFP expressing stable cell line (bottom left). Scale bar = 10 μm. (*B*) A representative image showed that the TXN2-GFP proteins (green) expressed in mitochondria. Mitochondria were visualized by the staining of MitoTracker (red). Scale bar = 2 μm. (*C* & *D*) Overexpression of TXN2 in differentiated myotubes inhibited H_2O_2-induced protein ubiquitination and the activation of caspase-3 (cleaved caspase-3). Differentiated myotubes with and without TXN2 were treated with H_2O_2 at 40 μM for 24 h. Protein lysates were then subjected to western blot analysis (*C*) and grey density was quantitated by ImageJ (*D*). Shown with $n = 2$, with three repeats, $^*P < 0.05$.

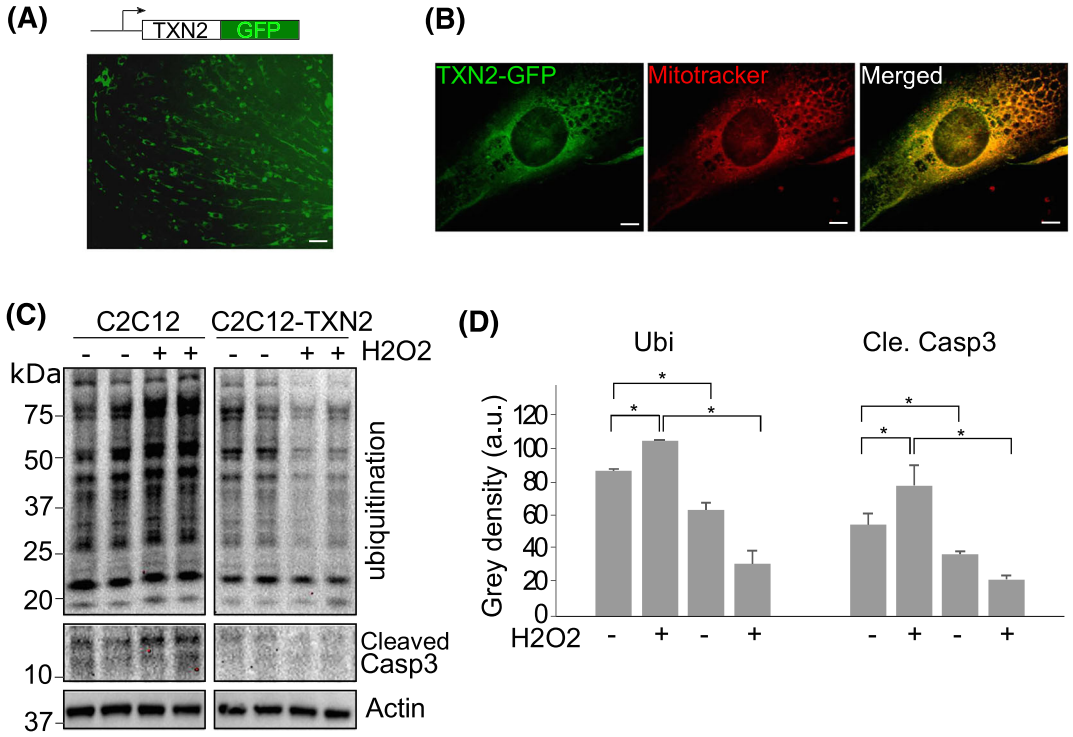

muscles) and upon fibre size (CSA). Therefore, TXN2 overexpression does not attenuate muscle loss following 14 days of denervation.

In vivo overexpression of TXN2 attenuates denervation-induced oxidative stress and apoptosis but does not suppress the activation of HDAC-myogenin and mTORC1-FoxO signalling

The failure of TXN2 overexpression to attenuate denervation-induced muscle atrophy suggests that the underlying mechanisms of muscle atrophy in denervation and ageing differ. It has been reported that ROS is induced in denervated muscle.[52] We found that denervation up-regulated ROS in control mice but not in TXN2-transgenic mice. (*Figure* 7A and 7B). This observation was further validated by the quantitative measurement of protein oxidation. The levels of DNP, nitrotyrosine, and 4HNE were induced in the denervated muscles of control mice, but they were not induced by denervation in the TXN2-overexpressing mice (*Figure* 7C). Also, the apoptotic markers, cleaved caspase-3, and caspase-9, were all up-regulated in denervated control muscles and were all successfully suppressed by TXN2 overexpression (*Figure* 7C). Therefore, TXN2 overexpression appears able to block oxidative stress and apoptosis after denervation, but it does not block muscle atrophy. This indicates that oxidative stress and its associated apoptotic changes may not be the major factors in acute denervation-induced muscle atrophy.

Protein polyubiquitination is a necessary step for 26S proteasome-mediated protein degradation, and an increased level of ubiquitinated proteins is a sign of accelerated protein degradation when the proteasome functions normally. We found that protein polyubiquitination increased in the denervated muscles in both control and TXN2-transgenic mice (*Figure* 7C).

We further examined upstream signals that are known to regulate protein metabolism and muscle mass, such as HDAC4/myogenin, FoxO, and mTORC1, at either the protein or mRNA levels. The activity of the mTORC1 signalling pathway, shown here by the ratio of the phosphorylated S6 protein to the total S6 protein (pS6/S6), is induced in the denervated muscle, and this denervation-dependent induc-

Figure 6 Overexpression of TXN2 does not attenuate the denervation-dependent reduction of muscle mass and size. (*A*) A schematic diagram to show the use of TXN2 transgenic mice to attenuate denervation-induced muscle atrophy through suppressing ROS generated in the denervated muscle. The sciatic nerve was sectioned and the hindlimb muscles were harvested 14 days post-denervation. (*B*) Overexpression of TXN2 did not attenuate denervation-dependent loss of muscle weight. Relative muscle weight was calculated as the ratio of the denervated muscle over the innervated muscle in control (Ctl), hemizygous (tg/+), and homozygous (tg/tg) mice. Both gastrocnemius muscle (Gastroc.) and tibialis anterior (TA) muscles were measured. $n = 3$, ns, no statistic difference. $^*P < 0.05$. (*B*) Overexpression of TXN2 did not attenuate the denervation-dependent reduction of muscle fibre size. Representative images of the cross-section of innervated (Inn) and denervated (Den) from control and TXN2-transgenic mice were shown (left). The cross-sectional area was measured by ImageJ software in the controls and the TXN2 homozygous mice. Approximately 250 fibres per region, three regions per sample, and three samples per group were measured. ns, no statistic difference, $^*P < 0.05$.

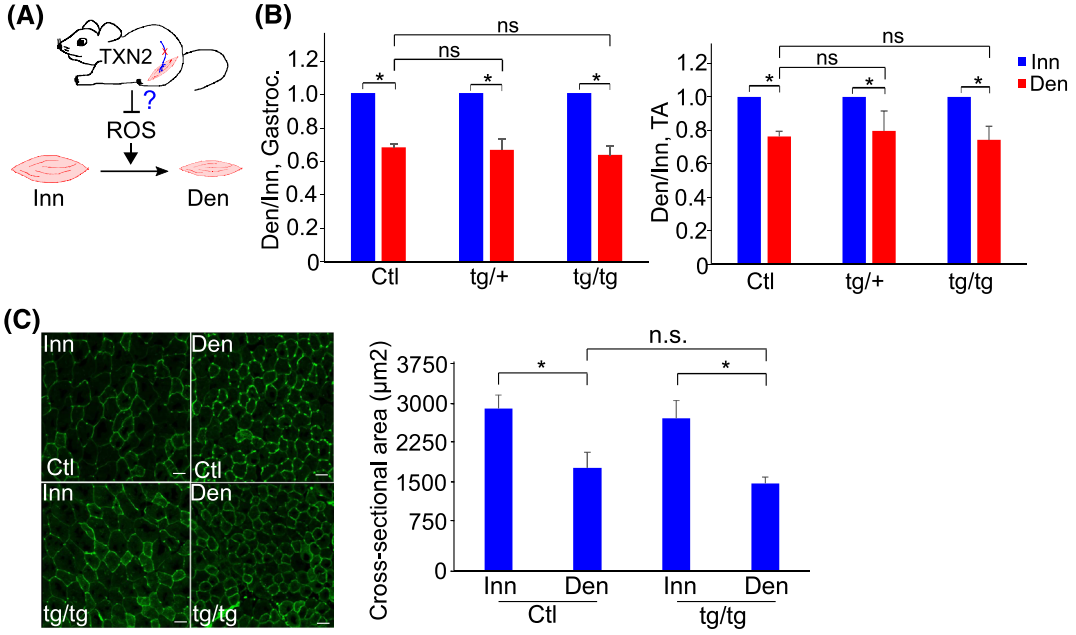

tion was not blocked in the TXN2-transgenic mice (*Figure* 7C). The mRNA expression of HDAC4, myogenin, FoxO1, and FoxO3 were also all significantly up-regulated in the denervated muscle in the control mice, as shown by quantitative PCR in *Figure* 7D, and overexpression did not suppress the denervation-dependent induction of these genes. Therefore, overexpressing TXN2 does not attenuate the activation of mTORC1-FoxO and HDAC4-Myogenin signalling pathways upstream of protein degradation in the denervated muscle, and this may explain the finding that TXN2 overexpression does not attenuate denervation atrophy.

To summarize, overexpressing TXN2 is sufficient to suppress oxidative stress and the associated apoptosis in denervated muscle. However, these do not appear to be the dominant upstream signals that activate protein degradation in acute denervation-induced neurogenic muscle atrophy, as overexpression of TXN2 does not prevent muscle loss in this model.

Discussion

Understanding the mechanisms that underlie muscle atrophy may help to develop interventions against age-related muscle loss and neurogenic muscle atrophy. Both oxidative stress and denervation occur in aged skeletal muscle and have been considered potential therapeutic targets in preventing age-related muscle loss. Using a transgenic mouse model that overexpresses the mitochondrial antioxidant TXN2, we report here that increased TXN2 attenuates oxidative stress and apoptotic changes in both denervated and aged skeletal muscle. However, while increased TXN2 attenuated muscle atrophy in our ageing model, it did not reduce muscle atrophy in the acute denervation model. This indicates that oxidative stress and its associated apoptotic changes play a more prominent role in age-related muscle atrophy than in acute denervation-induced atrophy and that TXN2-dependent attenuation of age-related muscle loss occurs primarily via inhibition of oxidative stress/apoptosis and unlikely via blockade of acute denervation-related pathways. TXN2-based therapy is thus a potential approach to reduce age-related atrophy and its associated morbidities.

This study represents the first to investigate the functional role of TXN2 in young and aged skeletal muscle. Constitutively expressed TXN2 did not alter the skeletal muscle phenotype during development. Therefore, increased levels of TXN2 appear not to alter the effect of physiological levels of ROS that are present up to early adulthood. This may be be-

DOI: 10.1002/rco2.57

Figure 7 Overexpression of TXN2 attenuates denervation-induced oxidative stress and apoptosis, but not the signalling pathways upstream of the ubiquitin-proteasome system. (*A* & *B*) Overexpression of TXN2 prevented denervation-induced ROS production in skeletal muscle tissues. ROS were stained with DHE (*A*) and the fluorescent intensity was quantitated by ImageJ software (*B*). Fold change of ROS was calculated as the ratio of denervation over innervation in control, hemizygous, and homozygous mice. n = 3 per group, $^*P < 0.05$. (*C*) TXN2 overexpression suppressed the denervation-dependent up-regulation of protein oxidation, apoptotic markers, but not myogenin and mTORC1 pathways. Left panel: western blot analysis was performed to examine the levels of protein expression. Right panel: the grey density of the detected protein bands was quantitated by ImageJ to show the levels of protein expression after normalized to the total protein (pons). a.u., arbitrary unit, n = 3 per group, $^*P < 0.05$. (*D*) Overexpression of TXN2 did not suppress denervation-induced gene expression of HDAC4, myogenin, and FoxO. Total RNAs were harvested from innervated and denervated (14 days) gastrocnemius muscles and subjected to quantitative PCR analysis. Fold change was calculated as the ratio of the denervated over the innervated. n = 3 per group, $^*P < 0.05$.

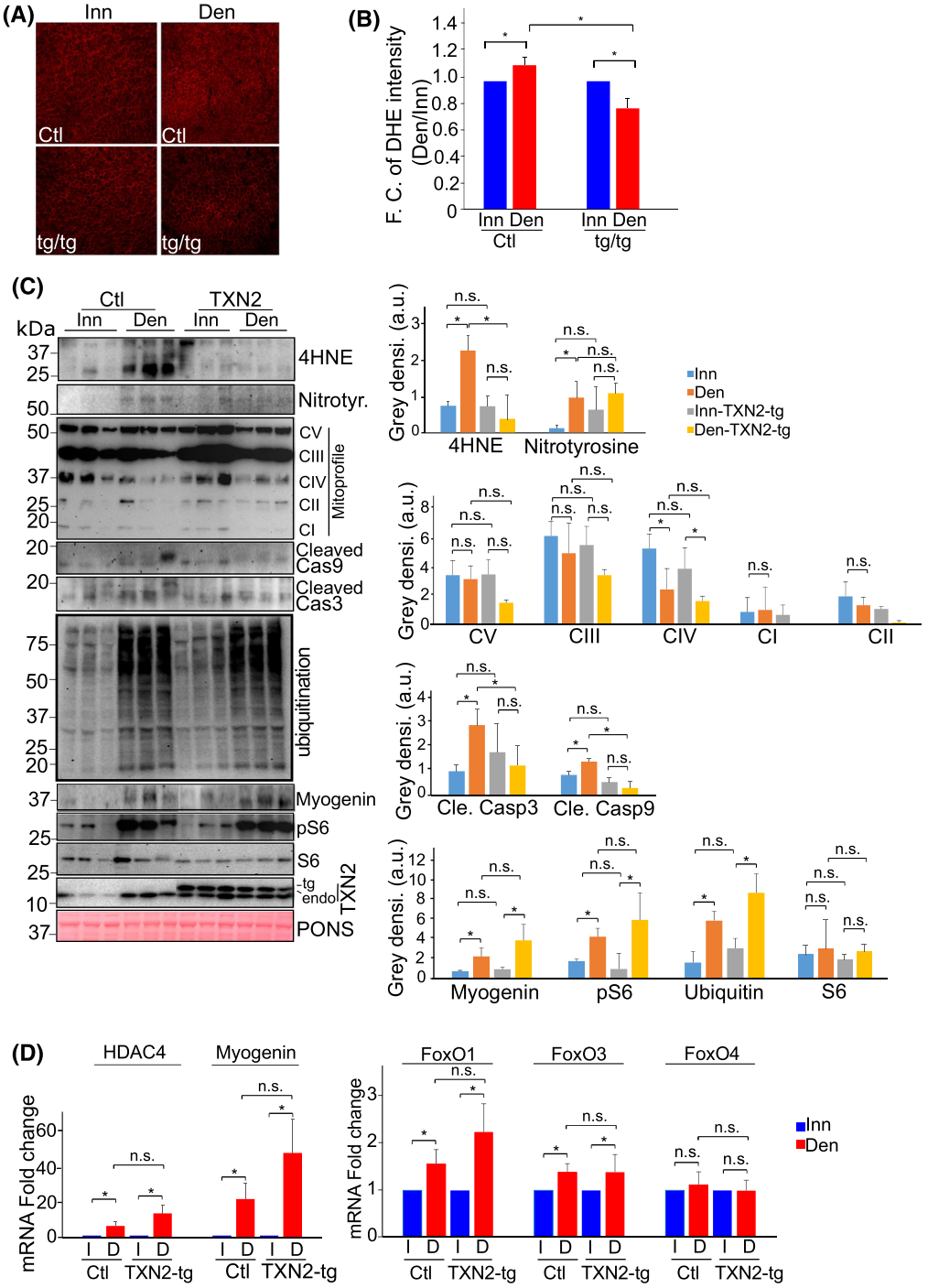

DOI: 10.1002/rco2.57

cause TXN2 functions as an indirect antioxidant by reducing Prx3, which is different from many other antioxidants (e.g. catalase and Trolox) that directly counteract ROS. Overexpressed TXN2 seems to suppress the excessive amount of ROS induced in ageing muscle, thereby attenuating age-dependent reduction of muscle mass and fibre size.

Although it has long been believed that MOS contributes to age-related muscle loss, the significance and the downstream effectors of oxidative stress in the ageing muscle remain controversial. Our data contribute the following key information to this field: (i) oxidative stress/apoptosis appears to be a key contributor to age-related muscle loss as both global mRNA profiling and focused signalling protein analysis show that oxidative stress/apoptosis increased in aged skeletal muscle and was suppressed by inhibition of oxidative stress, coincident with attenuation of ageing muscle loss; (ii) the major downstream effector of oxidative stress in ageing muscle appears to be mitochondrial apoptosis, as mitochondrial apoptotic signalling—cleaved caspase-9/3—was activated in aged skeletal muscle, and suppression of MOS by overexpressed mitochondrial TXN2 attenuated apoptosis and muscle fibre loss. Apoptotic muscle fibre death may result from a progressive accumulation of nuclear and cellular apoptotic changes over time, which ultimately leads to gradual, perhaps segmental, muscle fibre death, and loss during ageing.[53,54] Beyond apoptotic changes, our data also suggest that inhibition of protein oxidation and ubiquitination by TXN2 may help attenuate muscle protein degradation/atrophy and fibre loss in ageing.

In acute muscle denervation, overexpression of TXN2 inhibited oxidative stress and apoptosis, but not muscle atrophy. Interestingly, deficiency in BAX/BAK, or BAX alone, also suppressed denervation-induced oxidative stress and apoptosis,[55,56] but BAX/BAK deficiency was able to attenuate muscle atrophy.[56] This inconsistency may suggest that the downstream signallings of BAX/BAK and TXN2 are different, and BAX/BAK may have effectors other than mitochondrial apoptosis. It is also possible that the protective effect against muscle atrophy in BAX/BAK-deficient mice was observed at 7 days after denervation, whereas in TXN2 mice, the denervated muscles were examined at 14 days. It remains unclear but possible that oxidative stress and apoptosis may change the rate of muscle atrophy during denervation at early time points.

The aetiology of age-related muscle loss is complex, but it is well-documented that denervation is a subevent in ageing muscle and contributes to ageing muscle loss.[57] Denervation occurs in aged muscle, and denervation-dependent changes are in many respects similar to the changes seen in aged skeletal muscle—for example, increased ROS, oxidative stress, and apoptosis.[51,52] It has thus been hypothesized that age-related muscle loss is due in part to denervation and likely that MOS/apoptosis are signalling pathways common to each of these processes.[49] We, however, did not observe that TXN2 overexpression attenuates acute, denervation-induced muscle atrophy. Similarly, the antioxidant Trolox, when used to quench increased ROS in an acute muscle denervation model, did not attenuate muscle atrophy.[52] Failure to attenuate denervation-associated muscle atrophy by TXN2 overexpression and Trolox informs us that oxidative stress and associated apoptosis do not play a major role in acute muscle atrophy following denervation. Muscle loss in acute muscle denervation is likely mediated predominately by the ubiquitin-proteasome system–dependent protein degradation[58,59] rather than the oxidative stress-induced mitochondrial apoptosis. Consistent with this interpretation, signalling pathways upstream of ubiquitin-proteasome system, such as the FoxO[3,7] and HDAC/myogenin pathways,[4,5] were not significantly affected by TXN2 in the denervated muscle model (*Figure* 7).

Perhaps oxidative stress and apoptosis only emerge as major players in muscle atrophy resulting from chronic, long-term denervation. Because muscle ageing may in fact represent a form of chronic, long-term muscle denervation, the current findings cannot rule out the significance of chronic denervation in age-related muscle atrophy. In line with this, we cannot neither rule out nor prove the possibility that TXN2, or other antioxidants, benefits aged muscle through attenuating an effect resulting from long-term denervation in aged muscle. Future studies with denervation experiments in aged TXN2 mice would shed some light on this issue.

Lastly, although most reports support the view that oxidative stress is necessary for ageing muscle loss and functional decline, some studies argue that mitochondrial ROS *per se* may not be sufficient to induce age-related muscle atrophy. For example, muscle-specific deletion of SOD2 increased mitochondrial superoxide release and oxidative damage, elicited NMJ disruption and contractile abnormalities, but it did not accelerate age-related muscle atrophy.[60,61] Rather, this model exhibited a 10–15% increase in muscle mass, associated with increased central nuclei and branched fibres.[61] This appears to contradict the data from antioxidant overexpression and treatment.[29,30] One may address this controversy by appreciating the distinct composition of ROS in SOD knockout muscle and normal ageing muscle. Because SOD2 converts superoxide to H_2O_2, lack of SOD2 increases the accumulation of superoxide radicals but decreases the production of H_2O_2. Different species of ROS likely produce different effects on muscle: some may serve mainly as signalling molecules supporting regeneration, while others may primarily subserve protein oxidation and degradation.[62] ROS could be a double-edged sword,[63] and its net effects in ageing muscle may depend on both the levels and the composition of ROS. Given the possibility that the pathogenic effect of ROS may differ with the particular type of ROS species, it may be fruitful to investigate this type of ROS-species-specific effect in future work.

DOI: 10.1002/rco2.57

In summary, we have investigated the functional role of TXN2 in skeletal muscle during ageing and denervation, and we show that the causal factors in age-related muscle atrophy are different from those in acute denervation-induced muscle atrophy. Oxidative stress and apoptotic signalling play an important role in ageing muscle loss but not in acute denervation. It remains unclear if TXN2 protects the ageing muscle entirely by suppression of ROS-induced oxidative stress, as it also directly reduces other substrates (e.g. NFkB and HDAC4), beyond Prx3. Although the detailed mechanism of action of TXN2 remains to be elucidated, our findings with TXN2 overexpressing mice support the concept of mitochondrial-targeted antioxidants as promising candidates to attenuate age-related muscle loss.

Acknowledgements

We are grateful to Dr. Dean Jones (Emory University) for providing the TXN2 transgenic mouse line. We thank Ms. Donna Yoshida for her technical assistance. The authors certify that they comply with the ethical guidelines for publishing in the *Journal of Cachexia, Sarcopenia, and Muscle: update 2019*.

Conflict of interest

None declared.

Funding

This study was supported by a VA merit review grant.

Online supplementary material

Additional supporting information may be found online in the Supporting Information section at the end of the article.

Data S1. Supporting Information.

References

1. Santilli V, Bernetti A, Mangone M, Paoloni M. Clinical definition of sarcopenia. *Clin Cases Miner Bone Metab* 2014;**11**: 177–180.
2. Rommel C, Bodine SC, Clarke BA, Rossman R, Nunez L, Stitt TN, et al. Mediation of IGF-1-induced skeletal myotube hypertrophy by PI(3)K/Akt/mTOR and PI(3)K/Akt/GSK3 pathways. *Nat Cell Biol* 2001;**3**:1009–1013.
3. Tang H, Inoki K, Lee M, Wright E, Khuong A, Sugiarto S, et al. mTORC1 promotes denervation-induced muscle atrophy through a mechanism involving the activation of FoxO and E3 ubiquitin ligases. *Sci Signal* 2014;**7**:ra18.
4. Tang H, Macpherson P, Marvin M, Meadows E, Klein WH, Yang XJ, et al. A histone deacetylase 4/myogenin positive feedback loop coordinates denervation-dependent gene induction and suppression. *Mol Biol Cell* 2009;**20**:1120–1131.
5. Moresi V, Williams AH, Meadows E, Flynn JM, Potthoff MJ, McAnally J, et al. Myogenin and class II HDACs control neurogenic muscle atrophy by inducing E3 ubiquitin ligases. *Cell* 2010;**143**:35–45.
6. Cai D, Frantz JD, Tawa NE, Melendez PA, Oh BC, Lidov HG, et al. IKKbeta/NF-kappaB activation causes severe muscle wasting in mice. *Cell* 2004;**119**:285–298.
7. Sandri M, Sandri C, Gilbert A, Skurk C, Calabria E, Picard A, et al. Foxo transcription factors induce the atrophy-related ubiquitin ligase atrogin-1 and cause skeletal muscle atrophy. *Cell* 2004;**117**:399–412.
8. Tang H, Lee M, Budak MT, Pietras N, Hittinger S, Vu M, et al. Intrinsic apoptosis in mechanically ventilated human diaphragm: linkage to a novel Fos/FoxO1/Stat3-Bim axis. *FASEB J* 2011;**25**: 2921–2936.
9. Rossi P, Marzani B, Giardina S, Negro M, Marzatico F. Human skeletal muscle aging and the oxidative system: cellular events. *Curr Aging Sci* 2008;**1**:182–191.
10. Gomes MJ, Martinez PF, Pagan LU, Damatto RL, Cezar MDM, Lima ARR, et al. Skeletal muscle aging: influence of oxidative stress and physical exercise. *Oncotarget* 2017;**8**:20428–20440.
11. Szentesi P, Csernoch L, Dux L, Keller-Pintér A. Changes in redox signaling in the skeletal muscle with aging. *Oxid Med Cell Longev* 2019;**2019**:4617801.
12. McArdle A, Pollock N, Staunton CA, Jackson MJ. Aberrant redox signalling and stress response in age-related muscle decline: role in inter- and intra-cellular signalling. *Free Radic Biol Med* 2019;**132**:50–57.
13. Marzetti E, Calvani R, Cesari M, Buford TW, Lorenzi M, Behnke BJ, et al. Mitochondrial dysfunction and sarcopenia of aging: from signaling pathways to clinical trials. *Int J Biochem Cell Biol* 2013;**45**:2288–2301.
14. Aoi W, Sakuma K. Oxidative stress and skeletal muscle dysfunction with aging. *Curr Aging Sci* 2011;**4**:101–109.
15. Gianni P, Jan KJ, Douglas MJ, Stuart PM, Tarnopolsky MA. Oxidative stress and the mitochondrial theory of aging in human skeletal muscle. *Exp Gerontol* 2004;**39**: 1391–1400.
16. Gueugneau M, Coudy-Gandilhon C, Gourbeyre O, Chambon C, Combaret L, Polge C, et al. Proteomics of muscle chronological ageing in post-menopausal women. *BMC Genomics* 2014;**15**:1165.
17. Macpherson PC, Wang X, Goldman D. Myogenin regulates denervation-dependent muscle atrophy in mouse soleus muscle. *J Cell Biochem* 2011;**112**:2149–2159.
18. Dai DF, Chiao YA, Marcinek DJ, Szeto HH, Rabinovitch PS. Mitochondrial oxidative stress in aging and healthspan. *Longev Healthspan* 2014;**3**:6.
19. Liguori I, Russo G, Curcio F, Bulli G, Aran L, Della-Morte D, et al. Oxidative stress, aging, and diseases. *Clin Interv Aging* 2018; **13**:757–772.
20. Soendenbroe C, Heisterberg MF, Schjerling P, Karlsen A, Kjaer M, Andersen JL, et al. Molecular indicators of denervation in aging human skeletal muscle. *Muscle Nerve* 2019;**60**:453–463.
21. Aare S, Spendiff S, Vuda M, Elkrief D, Perez A, Wu Q, et al. Failed reinnervation in aging skeletal muscle. *Skelet Muscle* 2016;**6**:29.
22. Balice-Gordon RJ. Age-related changes in neuromuscular innervation. *Muscle Nerve Suppl* 1997;**5**:S83–S87.
23. Chai RJ, Vukovic J, Dunlop S, Grounds MD, Shavlakadze T. Striking denervation of neuromuscular junctions without lumbar motoneuron loss in geriatric mouse muscle. *PLoS ONE* 2011;**6**:e28090.

24. Valdez G, Tapia JC, Lichtman JW, Fox MA, Sanes JR. Shared resistance to aging and ALS in neuromuscular junctions of specific muscles. *PLoS ONE* 2012;**7**:e34640.
25. Valdez G, Tapia JC, Kang H, Clemenson GD, Gage FH, Lichtman JW, et al. Attenuation of age-related changes in mouse neuromuscular synapses by caloric restriction and exercise. *Proc Natl Acad Sci U S A* 2010;**107**:14863–14868.
26. Cox AG, Winterbourn CC, Hampton MB. Mitochondrial peroxiredoxin involvement in antioxidant defence and redox signalling. *Biochem J* 2009;**425**:313–325.
27. Ott M, Gogvadze V, Orrenius S, Zhivotovsky B. Mitochondria, oxidative stress and cell death. *Apoptosis* 2007;**12**:913–922.
28. Dai DF, Chiao YA, Martin GM, Marcinek DJ, Basisty N, Quarles EK, et al. Mitochondrial-targeted catalase: extended longevity and the roles in various disease models. *Prog Mol Biol Transl Sci* 2017;**146**:203–241.
29. Campbell MD, Duan J, Samuelson AT, Gaffrey MJ, Merrihew GE, Egertson JD, et al. Improving mitochondrial function with SS-31 reverses age-related redox stress and improves exercise tolerance in aged mice. *Free Radic Biol Med* 2019;**134**:268–281.
30. Javadov S, Jang S, Rodriguez-Reyes N, Rodriguez-Zayas AE, Soto Hernandez J, Krainz T, et al. Mitochondria-targeted antioxidant preserves contractile properties and mitochondrial function of skeletal muscle in aged rats. *Oncotarget* 2015;**6**:39469–39481.
31. Sakellariou GK, Pearson T, Lightfoot AP, Nye GA, Wells N, Giakoumaki II, et al. Mitochondrial ROS regulate oxidative damage and mitophagy but not age-related muscle fiber atrophy. *Sci Rep* 2016;**6**:33944.
32. Schriner SE, Linford NJ, Martin GM, Treuting P, Ogburn CE, Emond M, et al. Extension of murine life span by overexpression of catalase targeted to mitochondria. *Science* 2005;**308**:1909–1911.
33. Lee HY, Choi CS, Birkenfeld AL, Alves TC, Jornayvaz FR, Jurczak MJ, et al. Targeted expression of catalase to mitochondria prevents age-associated reductions in mitochondrial function and insulin resistance. *Cell Metab* 2010;**12**:668–674.
34. Dai DF, Santana LF, Vermulst M, Tomazela DM, Emond MJ, MacCoss MJ, et al. Overexpression of catalase targeted to mitochondria attenuates murine cardiac aging. *Circulation* 2009;**119**:2789–2797.
35. Radyuk SN, Rebrin I, Klichko VI, Sohal BH, Michalak K, Benes J, et al. Mitochondrial peroxiredoxins are critical for the maintenance of redox state and the survival of adult Drosophila. *Free Radic Biol Med* 2010;**49**:1892–1902.
36. Matthews JR, Wakasugi N, Virelizier JL, Yodoi J, Hay RT. Thioredoxin regulates the DNA binding activity of NF-kappa B by reduction of a disulphide bond involving cysteine 62. *Nucleic Acids Res* 1992;**20**:3821–3830.
37. Ago T, Liu T, Zhai P, Chen W, Li H, Molkentin JD, et al. A redox-dependent pathway for regulating class II HDACs and cardiac hypertrophy. *Cell* 2008;**133**:978–993.
38. Tanaka T, Hosoi F, Yamaguchi-Iwai Y, Nakamura H, Masutani H, Ueda S, et al. Thioredoxin-2 (TRX-2) is an essential gene regulating mitochondria-dependent apoptosis. *EMBO J* 2002;**21**:1695–1703.
39. Pirson M, Debrulle S, Clippe A, Clotman F, Knoops B. Thioredoxin-2 modulates neuronal programmed cell death in the embryonic chick spinal cord in basal and target-deprived conditions. *PLoS ONE* 2015;**10**:e0142280.
40. Pérez VI, Lew CM, Cortez LA, Webb CR, Rodriguez M, Liu Y, et al. Thioredoxin 2 haploinsufficiency in mice results in impaired mitochondrial function and increased oxidative stress. *Free Radic Biol Med* 2008;**44**:882–892.
41. Nonn L, Williams RR, Erickson RP, Powis G. The absence of mitochondrial thioredoxin 2 causes massive apoptosis, exencephaly, and early embryonic lethality in homozygous mice. *Mol Cell Biol* 2003;**23**:916–922.
42. Huang Q, Zhou HJ, Zhang H, Huang Y, Hinojosa-Kirschenbaum F, Fan P, et al. Thioredoxin-2 inhibits mitochondrial reactive oxygen species generation and apoptosis stress kinase-1 activity to maintain cardiac function. *Circulation* 2015;**131**:1082–1097.
43. Svensson MJ, Larsson J. Thioredoxin-2 affects lifespan and oxidative stress in Drosophila. *Hereditas* 2007;**144**:25–32.
44. He M, Cai J, Go YM, Johnson JM, Martin WD, Hansen JM, et al. Identification of thioredoxin-2 as a regulator of the mitochondrial permeability transition. *Toxicol Sci* 2008;**105**:44–50.
45. Li YY, Xiang Y, Zhang S, Wang Y, Yang J, Liu W, et al. Thioredoxin-2 protects against oxygen-glucose deprivation/reperfusion injury by inhibiting autophagy and apoptosis in H9c2 cardiomyocytes. *Am J Transl Res* 2017;**9**:1471–1482.
46. Holzerova E, Danhauser K, Haack TB, Kremer LS, Melcher M, Ingold I, et al. Human thioredoxin 2 deficiency impairs mitochondrial redox homeostasis and causes early-onset neurodegeneration. *Brain* 2016;**139**:346–354.
47. Sugano E, Murayama N, Takahashi M, Tabata K, Tamai M, Tomita H. Essential role of thioredoxin 2 in mitigating oxidative stress in retinal epithelial cells. *J Ophthalmol* 2013;**2013**:185825.
48. Willadt S, Nash M, Slater C. Age-related changes in the structure and function of mammalian neuromuscular junctions. *Ann N Y Acad Sci* 2018;**1412**:41–53.
49. Muller FL, Song W, Jang YC, Liu Y, Sabia M, Richardson A, et al. Denervation-induced skeletal muscle atrophy is associated with increased mitochondrial ROS production. *Am J Physiol Regul Integr Comp Physiol* 2007;**293**:R1159–R1168.
50. O'Leary MF, Hood DA. Denervation-induced oxidative stress and autophagy signaling in muscle. *Autophagy* 2009;**5**:230–231.
51. Abruzzo PM, di Tullio S, Marchionni C, Belia S, Fanó G, Zampieri S, et al. Oxidative stress in the denervated muscle. *Free Radic Res* 2010;**44**:563–576.
52. Pigna E, Greco E, Morozzi G, Grottelli S, Rotini A, Minelli A, et al. Denervation does not induce muscle atrophy through oxidative stress. *Eur J Transl Myol* 2017;**27**:6406.
53. Cheema N, Herbst A, McKenzie D, Aiken JM. Apoptosis and necrosis mediate skeletal muscle fiber loss in age-induced mitochondrial enzymatic abnormalities. *Aging Cell* 2015;**14**:1085–1093.
54. Dupont-Versteegden EE. Apoptosis in muscle atrophy: relevance to sarcopenia. *Exp Gerontol* 2005;**40**:473–481.
55. Siu PM, Alway SE. Deficiency of the Bax gene attenuates denervation-induced apoptosis. *Apoptosis* 2006;**11**:967–981.
56. O'Leary MF, Vainshtein A, Carter HN, Zhang Y, Hood DA. Denervation-induced mitochondrial dysfunction and autophagy in skeletal muscle of apoptosis-deficient animals. *Am J Physiol Cell Physiol* 2012;**303**:C447–C454.
57. Park KH. Mechanisms of muscle denervation in aging: insights from a mouse model of amyotrophic lateral sclerosis. *Aging Dis* 2015;**6**:380–389.
58. Bodine SC, Latres E, Baumhueter S, Lai VK, Nunez L, Clarke BA, et al. Identification of ubiquitin ligases required for skeletal muscle atrophy. *Science* 2001;**294**:1704–1708.
59. Gomes MD, Lecker SH, Jagoe RT, Navon A, Goldberg AL. Atrogin-1, a muscle-specific F-box protein highly expressed during muscle atrophy. *Proc Natl Acad Sci U S A* 2001;**98**:14440–14445.
60. Lustgarten MS, Jang YC, Liu Y, Qi W, Qin Y, Dahia PL, et al. MnSOD deficiency results in elevated oxidative stress and decreased mitochondrial function but does not lead to muscle atrophy during aging. *Aging Cell* 2011;**10**:493–505.
61. Ahn B, Ranjit R, Premkumar P, Pharaoh G, Piekarz KM, Matsuzaki S, et al. Mitochondrial oxidative stress impairs contractile function but paradoxically increases muscle mass via fibre branching. *J Cachexia Sarcopenia Muscle* 2019;**10**:411–428.
62. Sullivan LB, Chandel NS. Mitochondrial reactive oxygen species and cancer. *Cancer Metab* 2014;**2**:17.
63. Kalogeris T, Bao Y, Korthuis RJ. Mitochondrial reactive oxygen species: a double edged sword in ischemia/reperfusion vs preconditioning. *Redox Biol* 2014;**2**:702–714.